



## IMPACT OF THE CATALYST BASICITY ON THE MECHANISM OF OCM REACTION PERFORMED OVER ALKALINE EARTH –Nd<sub>2</sub>O<sub>3</sub> MIXED OXIDES

Florica PAPA,<sup>a\*</sup> Dana GINGAȘU,<sup>a</sup> Luminița PATRON,<sup>a</sup> Akane MIYAZAKI<sup>b</sup> and Ioan BALINT<sup>a</sup>

<sup>a</sup> Institute of Physical Chemistry of the Roumanian Academy, Spl. Independentei 202, Bucharest 060021, Roumania

<sup>b</sup> Department of Chemical and Biological Sciences, Faculty of Science, Japan Women's University, 2-8-1 Mejirodai, Bunkyo-ku, Tokyo 112-8681, Japan

Received February 12, 2010

The oxidative coupling of methane (OCM) and the associate reaction mechanism for C<sub>2</sub><sup>+</sup> formation over an equimolecular mixture of alkaline earth oxides (BeO, MgO, CaO and SrO) with Nd<sub>2</sub>O<sub>3</sub> was investigated.

The equimolecular mixture of alkaline earth oxides with Nd<sub>2</sub>O<sub>3</sub> catalyst was investigated by X-ray diffraction (XRD), temperature programmed desorption (TPD) and infrared spectra IR methods.

The concentration of surface basic sites contributing to the formation of C<sub>2</sub><sup>+</sup> was determined by measuring the amount of evolved CO<sub>2</sub> in the 300 – 820 °C temperature range. The turnover frequency (TOF) and the activation energy values were calculated by quantitatively determining the total number basic sites retaining CO<sub>2</sub>.

### INTRODUCTION

The basicity of oxide catalyst has been found to be a key factor in determining the activity for hydrocarbon generation. Since the basic sites have been suggested to play an essential role in OCM reaction, a closer look on their properties would be useful. The combination between alkaline earth oxides with lanthanide oxides proved to be efficient OCM catalysts. For example, the catalytic activity of cation (Mg<sup>2+</sup>, Sr<sup>2+</sup>, Ni<sup>2+</sup>, Mn<sup>3+</sup>, <sup>4+</sup>, Zr<sup>4+</sup>) doped Nd<sub>2</sub>O<sub>3</sub> was already investigated to some extent because of the interesting catalytic properties showed for OCM reaction.<sup>1-3</sup> The good catalytic performances of alkaline earth oxides have been attributed mostly to their strong alkaline sites.<sup>4</sup> Nd<sub>2</sub>O<sub>3</sub> has been found also to contain medium and strong basic sites.<sup>5</sup> The effect of the insertion of the MgO, CaO, SrO, BaO into the host lattice of the Nd<sub>2</sub>O<sub>3</sub> was investigated by Filkova *et al.*<sup>6</sup> The combination between the high basicity and good incorporation of strontium into Nd<sub>2</sub>O<sub>3</sub> lattice

was considered to be responsible for the good catalytic activity showed for OCM reaction. The presence of strong strontium basic sites together with the incorporation into Nd<sub>2</sub>O<sub>3</sub> lattice was considered to explain the high C<sub>2</sub><sup>+</sup> selectivity of the mixed oxides. In a recently published work, the catalytic behavior for oxidative conversion of methane in reducing conditions (oxidative coupling of methane) was investigated for the first time over pure and neodymium substituted zinc ferrites prepared by combustion method.<sup>7</sup>

The analyzing an eventual quantitative relationship existing between the basic properties of oxide materials and the active sites for methane activation are no published works.

The aim of this paper is catalytic behavior of equimolecular mixture of alkaline earth oxides (BeO, MgO, CaO and SrO) with Nd<sub>2</sub>O<sub>3</sub> catalyst in OCM reaction and the quantitative relationship between the basic properties of these oxide materials and the active sites in coupling oxidative reaction of methane.

\* Corresponding author: frusu@icf.ro

## EXPERIMENTAL

The type mixed oxides  $\text{MO-Nd}_2\text{O}_3$  ( $\text{M} = \text{Be}, \text{Mg}, \text{Ca}, \text{Sr}$ ) were prepared starting from the tartarate complexes of the metals. The complex precursors were synthesized by separately dissolving the metal nitrate and tartaric acid in minimum amounts of distilled water followed by the mixing of the resulted solutions. The molar ratio between  $\text{M}^{n+}$  and tartaric ion was in most cases one to four. The solutions containing the mixtures of complex metal tartarates were slowly heated and kept at  $80^\circ\text{C}$  for 1 h. After cooling to room temperature, ethanol was added and then the pH was adjusted to 5.5–6 by using a solution of ammonium hydroxide in ethanol (1:1). The resulted light-yellow precipitates were maintained in liquid phase at  $4^\circ\text{C}$  for 24 h, filtered, washed several times with ethanol and finally dried on  $\text{P}_4\text{O}_{10}$ . In all cases, the formation of insoluble heteropolynuclear complexes, having the general formula  $(\text{NH}_4)_x[\text{MNd}_2(\text{Ta})_4(\text{OH})_y] \cdot \text{H}_2\text{O}$  ( $\text{M} = \text{Be}, \text{Mg}, \text{Ca}, \text{Sr}$ ), allowed an efficient mixing of component metal ions in the final oxide materials. The above-mentioned formulas were determined by elemental analysis. By using this preparation method, the washing out of component elements in preparation stage can be ruled out. The final step consisted in the air calcination of the precipitates at  $800^\circ\text{C}$  for 2 h.

Activity tests for OCM reaction were performed at atmospheric pressure with 0.1 g of catalyst (0.3 - 0.8-mm fraction) loaded in a tubular quartz microreactor (i.d. = 8 mm). The reactant gaseous mixtures were prepared using electronic flow controllers (Aalborg). The typical total flow rates of the reaction mixtures were  $24 \text{ cm}^3/\text{min}$  STP (standard temperature and pressure) for OCM reaction. The corresponding GHSV (gas hourly space velocity)  $14,400 \text{ h}^{-1}$ . The composition of reaction mixtures were 41.6%  $\text{CH}_4$ , 8.4%  $\text{O}_2$  ( $\text{CH}_4/\text{O}_2 = 5/1$ ) in Ar. The  $\text{O}_2$ ,  $\text{CH}_4$  were separated and analyzed by using a molecular sieve 13X column whereas

$\text{CO}_2$ ,  $\text{C}_2\text{H}_6$  and  $\text{C}_2\text{H}_4$  were determined on a Hayasept column (Buck Scientific - gas chromatograph).

The crystalline structure of the prepared samples was analyzed with a Rigaku Multiflex diffractometer provided with peak assignment software using  $\text{Cu K}\alpha$  radiation ( $\lambda = 1.54050 \text{ \AA}$ ).

Temperature programmed desorption (TPD) experiments were carried out in a flow system, Ar carrier with 0.1 g of catalyst, by using a ChemBET 3000-Quantachrome Instruments type apparatus equipped with thermal conductivity detectors (TCD). The typical heating rate was  $10^\circ\text{C} / \text{min}^{-1}$  and the total flow rate of the oxidizing or reducing gaseous mixtures was  $70 \text{ ml min}^{-1}$ . A mass spectrometer attached to the outlet confirmed that only  $\text{CO}_2$  evolved from the sample. The IR spectra were recorded on KBr pellets with a JASCO FT-IR 4100 spectrophotometer in the  $4000\text{--}400 \text{ cm}^{-1}$  range.

## RESULTS AND DISCUSSION

According to XRD data, presented in Fig. 1 the presence alkaline earth-oxides favored the formation of a well-crystallized hexagonal structure for  $\text{Nd}_2\text{O}_3$ . The hexagonal form of neodymia was found to perform better as OCM catalyst than the mixture of ordered cubic and hydrated phase of  $\text{Nd}_2\text{O}_3$ <sup>8</sup>. The characteristic XRD lines of alkaline earth-oxides are either missing ( $\text{MgO-Nd}_2\text{O}_3$ ) or are very weak (i. e.  $\text{BeO-Nd}_2\text{O}_3$ ,  $\text{CaO-Nd}_2\text{O}_3$  and  $\text{SrO-Nd}_2\text{O}_3$ ).

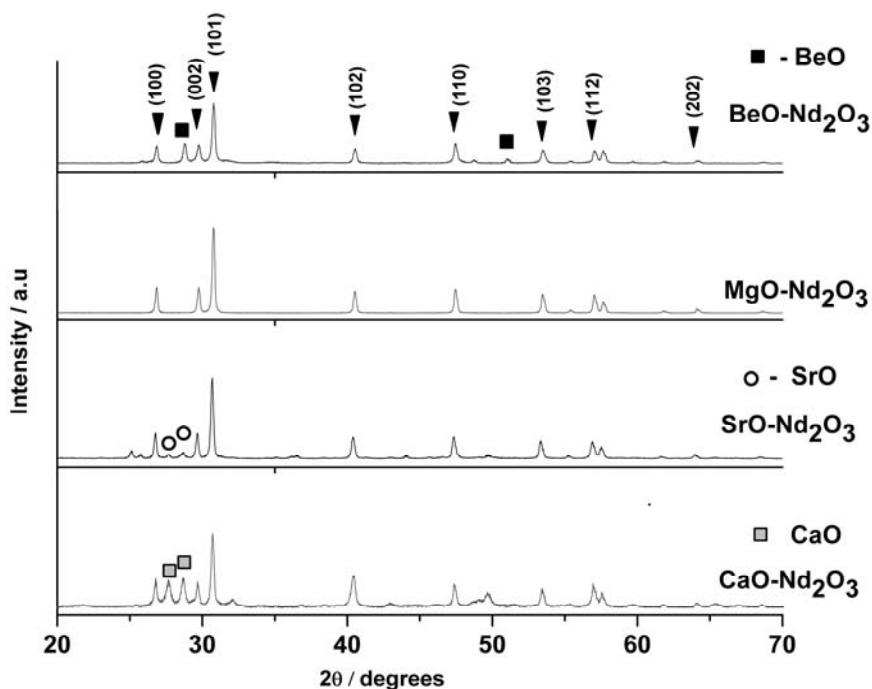


Fig. 1 – Comparative XRD spectra of  $\text{MO-Nd}_2\text{O}_3$  ( $\text{M} = \text{Be}, \text{Mg}, \text{Ca}, \text{Sr}$ ) compounds  
 ▼ -  $\text{Nd}_2\text{O}_3$ ; ■ -  $\text{BeO}$ ; □ -  $\text{CaO}$ ; ○ -  $\text{SrO}$ .

The yield of OCM reaction to  $C_2^+$  vs. temperature over the investigated oxide mixture is presented in Table 1. In all cases, the  $Y(C_2^+)$  showed a progressive increase with increasing the reaction temperature up to maxima at 775 °C. For  $T > 775$  °C the reaction yield to  $C_2^+$  hydrocarbons decreased, probably because of kinetic limitation. As can be seen in Table 1, the order of catalytic activity for hydrocarbon production at 775 °C was  $Ca > Mg > Sr > Be$ .

The selectivity to  $CO_2$  ( $CO_2$  levels as a function of reaction temperature) for the investigated oxide catalysts show a little dependency on reaction temperature. The formation of  $CO_2$  takes place at the lowest OCM reaction temperatures by consuming most of the oxygen from reaction mixture, the concentration of  $CO_2$  remaining afterward almost unchanged.

The comparative TPD profiles of spent mixed oxides are shown Fig. 2. The  $CO_2$  desorption peaks observed in the case of  $BeO-Nd_2O_3$  (at 528 and 639 °C) and  $MgO-Nd_2O_3$  (at 606 and 668 °C) are consistent with different types  $CO_2$  retained by the alkaline sites of mixed oxides. In the case of

$CaO-Nd_2O_3$ , only one large desorption peak could be observed at 678 °C. The TPD spectrum of  $SrO-Nd_2O_3$  exhibits a low temperature  $CO_2$  peak at 621 °C and a desorption peak located beyond highest temperature (820 °C) used in our measurements. The second observation is that the  $CO_2$  desorption maxima are shifted to higher temperatures as the basicity of alkaline earth oxide increased from beryllium to strontium.<sup>9</sup>

The quantities of desorbed  $CO_2$ , calculated by integration of the surface area under TPD curves of Fig.2, are listed in Table 1. The total amount of desorbed  $CO_2$  up to 820 °C, reflecting the basicity of the alkaline-earth oxides, increased from beryllium (0.24 mmol  $g^{-1}$ ), magnesium (1.15 mmol  $g^{-1}$ ) to calcium (2.2 mmol  $g^{-1}$ ). The lower amount of desorbed  $CO_2$  from  $SrO-Nd_2O_3$  (1.33 mmol  $g^{-1}$ ) compared to  $CaO-Nd_2O_3$  can be explained by the higher stability of carbonate species on to the surface of strontium oxide. Thus, significant amount of carbonate remaining undecomposed on the surface at the end of TPD run.

Table 1

The catalytic performances (conversions, selectivity and yields to  $C_2^+$ ) showed by alkaline-earth- $Nd_2O_3$  mixed oxides for OCM reaction at 775 °C

Catalysts	$X(CH_4)$ / %	$S(C_2^+)$ / %	$Y(C_2^+)_{max}$ / %
$BeO-Nd_2O_3$	21.28	40.71	8.66
$MgO-Nd_2O_3$	21.38	48.74	10.44
$CaO-Nd_2O_3$	23.08	51.97	11.78
$SrO-Nd_2O_3$	20.43	49.24	10.20

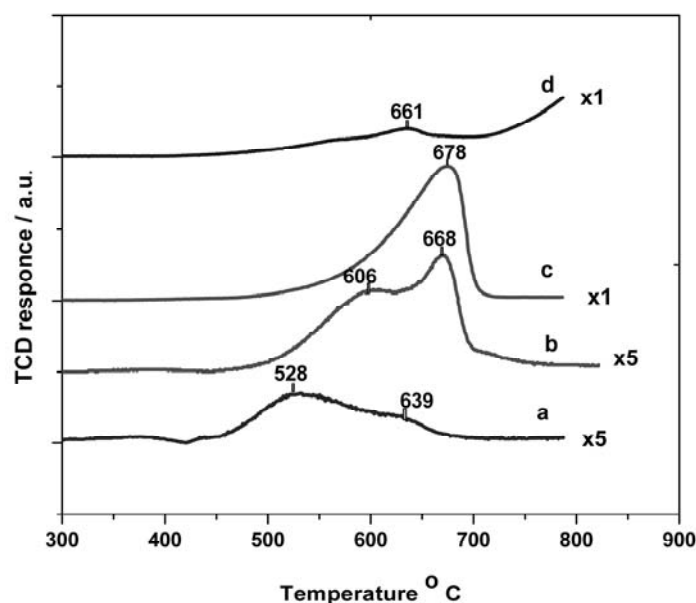


Fig. 2 – TPD spectra of  $CO_2$  evolved from  $MO-Nd_2O_3$  ( $M=Be, Mg, Ca, Sr$ ) oxide catalysts used in OCM reaction, a- $BeO-Nd_2O_3$ , b- $MgO-Nd_2O_3$ , c- $CaO-Nd_2O_3$ , d- $SrO-Nd_2O_3$ .

Table 2

The amount of surface carbonate removed from the surface of mixed oxides up to 820 °C and the physical surface area (BET)

Catalysts	Amount of surface carbonate / mmol	
	CO <sub>2</sub> g <sup>-1</sup>	S <sub>BET</sub> / m <sup>2</sup> g <sup>-1</sup>
BeO-Nd <sub>2</sub> O <sub>3</sub>	0.24	7.1
MgO-Nd <sub>2</sub> O <sub>3</sub>	1.15	6.5
CaO-Nd <sub>2</sub> O <sub>3</sub>	2.2	6.0
SrO-Nd <sub>2</sub> O <sub>3</sub>	1.33	6.4

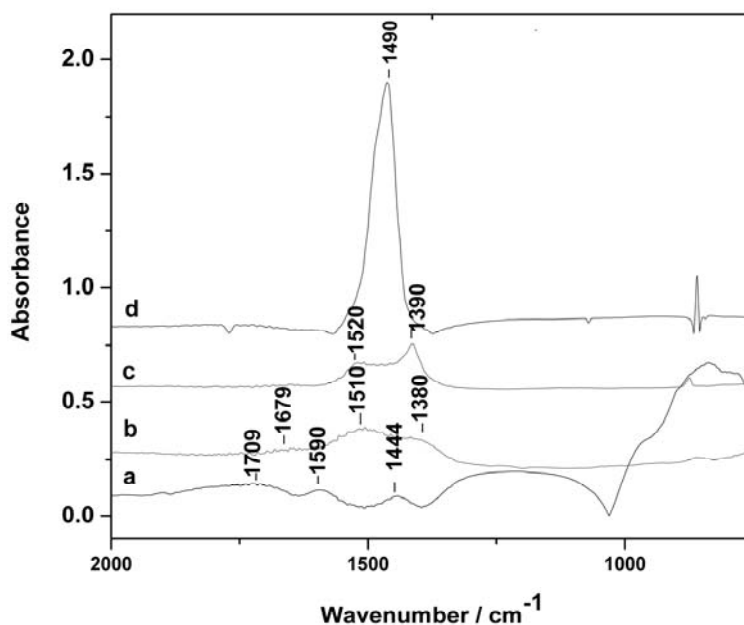


Fig. 3 – Comparative IR spectra of the MO–Nd<sub>2</sub>O<sub>3</sub> oxides (M = Be, Mg, Ca and Sr).  
a- BeO-Nd<sub>2</sub>O<sub>3</sub>, b-MgO- Nd<sub>2</sub>O<sub>3</sub>, c-CaO- Nd<sub>2</sub>O<sub>3</sub>, d-SrO- Nd<sub>2</sub>O<sub>3</sub>.

Table 3

Comparative IR results of the MO-Nd<sub>2</sub>O<sub>3</sub> oxides (M= Be, Mg, Ca and Sr)

	Carbonate species	Wave number /cm <sup>-1</sup>
BeNd <sub>2</sub> O <sub>4</sub>	bidentate	1709
	unidentate	1590, 1444
MgNd <sub>2</sub> O <sub>4</sub>	unidentate	1510, 1380
	bidentate	1679,
CaNd <sub>2</sub> O <sub>4</sub>	unidentate	1520, 1390
	bidentate	1645
SrNd <sub>2</sub> O <sub>4</sub>	monodentate and bidentate	1490 (broad peak)

The IR results confirmed the presence of carbonate species on the investigated oxide materials. The surface carbonate species formed on the surface of MO-Nd<sub>2</sub>O<sub>3</sub> mixed oxides were investigated by IR spectroscopy. Fig. 3 presents the IR spectra of the mixed oxides used in OCM reaction.

Table 3 presents the IR results of the mixed oxides used in OCM reaction. IR bands characteristic for different surface carbonate

species could be identified in the 1380 – 1708 cm<sup>-1</sup> region for all the investigated oxides.

Thus, the peak at 1709 can be assigned to CO<sub>2</sub> adsorbed on Nd<sub>2</sub>O<sub>3</sub><sup>10</sup> whereas the other two peaks can be attributed to the carbonate species located on the alkaline sites of MO. In the case of MO-Nd<sub>2</sub>O<sub>3</sub>, (M= Be, Mg, Ca) three characteristic IR band have been observed around of values 1400, 1500 and 1700 cm<sup>-1</sup>. Thus, it can be assumed that the surface carbonate species are more or less

related to the alkalinity of MO. On simple MO, the characteristic IR bands at 1500 and 1400  $\text{cm}^{-1}$  are characteristic to unidentate  $\text{CO}_2$  whereas the bidentate carbonate species are characterized by an IR band at 1670  $\text{cm}^{-1}$ .<sup>11</sup> SrO-Nd<sub>2</sub>O<sub>3</sub> sample shows only one broad IR band with the maxima located at 1490  $\text{cm}^{-1}$ . The main IR bands of carbonate species on SrF<sub>2</sub>/Nd<sub>2</sub>O<sub>3</sub> surface were detected at 1420 and 1520  $\text{cm}^{-1}$ .<sup>12</sup> From the surface area of the IR peak attributable to carbonate species, it can be said that the largest amount of carbonate is formed on SrO-Nd<sub>2</sub>O<sub>3</sub>. It is also clear that the broad IR band at 1490  $\text{cm}^{-1}$  contains the characteristic vibration of both, monodentate and bidentate carbonates.

According to IR results, (i) monodentate as well as bidentate carbonate species is formed on the surface of all mixed oxides, (ii) the alkaline earth oxides are mostly responsible for the formation of surface carbonate species and (iii) the amount of surface carbonate correlates well with the basicity of the alkaline earth oxide, increasing from BeO to SrO.

The concentration of surface basic sites contributing to the formation of  $\text{C}_2^+$  was determined by quantitatively measuring the amount of desorbed  $\text{CO}_2$  in the 300 – 820 °C temperature range. The amount of surface basicity correlates well with the catalytic activity for  $\text{C}_2^+$  production (at 775 °C) for all the investigated mixed oxides. The material showing the higher basicity (CaO-Nd<sub>2</sub>O<sub>3</sub>) in term of capacity of retaining removable  $\text{CO}_2$  showed the best performances for  $\text{C}_2^+$  production. It should be emphasized that the surface carbonate originates from the history of material preparation (tartarates are used as oxide precursors) as well as from the  $\text{CO}_2$  resulted from the unselective oxidation of  $\text{CH}_4$ .

The formation of  $\text{C}_2^+$  starts at the moment when the basic sites become available as a result of  $\text{CO}_2$  desorption. According to TPD results in fig. 2, the desorption of  $\text{CO}_2$  starts at  $T > 500$  °C. This correlates well with the beginning of  $\text{C}_2^+$  formation at  $T \geq 525$  °C.

Table 4

The rate of  $\text{C}_2^+$  formation over MO-Nd<sub>2</sub>O<sub>3</sub> mixed oxides (M=Be, Mg, Ca, Sr), the associated TOF at 775 °C and the activation energy values

Catalysts	Rate of $\text{C}_2^+$ formation /mol s <sup>-1</sup> g <sub>cat</sub> <sup>-1</sup>	TOF ( $\text{C}_2^+$ ) /s <sup>-1</sup>	Ea /Kcal/mol	
			a	b
BeO-Nd <sub>2</sub> O <sub>3</sub>	$1.82 \times 10^{-6}$	0.126	8.4	5
MgO-Nd <sub>2</sub> O <sub>3</sub>	$2.60 \times 10^{-6}$	0.037	11.2	14.3
CaO-Nd <sub>2</sub> O <sub>3</sub>	$2.37 \times 10^{-6}$	0.017	15	17
SrO-Nd <sub>2</sub> O <sub>3</sub>	$2.24 \times 10^{-6}$	0.028	2	9.2

<sup>a</sup> The activation energies calculated from the slopes of the  $\ln(\text{TOF}(\text{C}_2^+))$  vs  $1/T$  plots

<sup>b</sup> The apparent activation energies calculated from slopes of the  $\ln(\text{rate of } \text{C}_2^+)$  vs  $1/T$  plots

The reaction rates as well as the TOF (turnover frequency) values for  $\text{C}_2^+$  formation at 775 °C over the investigated mixed oxides are presented in Table 3. The TOF values were calculated by dividing the experimentally measured reaction rates (see Table 3) to number of basic sites responsible for  $\text{C}_2^+$  formation. It should be emphasized that this is the first attempt ever made to estimate the TOF values of  $\text{C}_2^+$  formation over oxide catalysts. Studies reporting on the determination of hydrocarbon oxidation TOF on metal oxides are very scarce. The main difficulties consisted in the identification of active sites and in finding reliable experimental methods for measuring their concentration. The TOF values for methane partial oxidation over Ru supported on

Ta<sub>2</sub>O<sub>5</sub>-ZrO<sub>2</sub> and Nb<sub>2</sub>O<sub>5</sub>-ZrO<sub>2</sub> at 500 °C ranged between 2.1 and 2.8 s<sup>-1</sup>.<sup>13</sup> In this case, the catalytic active sites have been determined by CO chemisorptions.

The variation of TOF values with the nature of alkaline-earths combined with Nd<sub>2</sub>O<sub>3</sub> is presented in Table 4. The TOF minimum was observed for CaO-Nd<sub>2</sub>O<sub>3</sub> and the highest one was determined for BeO-Nd<sub>2</sub>O<sub>3</sub>. High concentration of alkaline sites (i. e. the case of CaO-Nd<sub>2</sub>O<sub>3</sub>) gave lower TOF for  $\text{C}_2^+$  formation. The synergistic effect between the alkaline earth oxides and Nd<sub>2</sub>O<sub>3</sub> may be also an important factor mediating a complex relationship between concentration, strength of alkaline active and TOF for  $\text{C}_2^+$  production.

The activation energies were determined from the slopes of the logarithmic plots of TOF or rate of  $C_2^+$  formation vs.  $1/T$ .

Comparative values of the activation energies and apparent activation energies of mixed oxide are presented in Table 4. The values of apparent activation energies obtained from the rate of  $C_2^+$  formation are greater than values of obtained from TOF data. The order of values of activation energies for  $C_2^+$  formation is  $BeO-Nd_2O_3 < MgO-Nd_2O_3 < CaO-Nd_2O_3 < SrO-Nd_2O_3$ . This values presented in the table 4 is in a relative good agreement with the data reported in literature.<sup>14,15</sup>

### CONCLUSIONS

Our experimental results support also the idea that methane is converted to products on two types of active sites by independent pathways. The alkaline active sites (A) responsible for  $C_2^+$  formation are inactive at low temperature because they are blocked by  $CO_2$ . By raising the reaction temperatures these sites start to be progressively available for methane activation because of  $CO_2$  desorption. The concentration of available active sites at a given reaction temperature is dependent on the thermal stability of surface carbonate. The formation of  $CO_2$  product takes place on B type sites showing no interaction with  $CO_2$ . Thus the production of  $CO_2$ , starting at low temperatures, is relatively independent on reaction temperature.

*Acknowledgments.* Finance support by grant AMAP 32116 - CNMP is greatly acknowledged.

### REFERENCES

1. S.H. Lee., D. W. Jung, J.B. Kim, Y.-R. Kim, *Appl. Catal. A Gen.*, **1997**, *164*, 159-169.
2. D.G. Filkova, L.A. Petrov, M.Y. Sinev, Y.P. Tyulenin, *Catal. Lett.*, **1992**, *13*, 323-329.
3. G. Gayko, D. Wolf, E.V. Kondratenko, M. Baerns, *J.Catal.*, **1998**, *178*, 441-449.
4. V. R. Choudhary, V. H. Rane, R. V. Gadre, *J. Catal.*, **1994**, *145*, 300-311.
5. S. Kus, M. Otremba, M. Taniowski, *Fuel*, **2003**, *82*, 1331-1338.
6. D. Filkova, D. Wolf, G. Gayko, M. Baerns, L. Petrov, *Appl. Catal. A Gen.*, **1997**, *159*, 33-44.
7. F. Papa, L. Patron, O.Carp, C. Paraschiv, I. Balint, *J. Mol. Catal.*, **2009**, *299*, 93-97.
8. A. Burrows, C. J. Kiely, J. S. J. Hargreaves, R. W. Joyner, G. J. Hutchings, M. Y. Sinev, Y. P. Tulenin, *J. Catal.*, **1998**, *173*, 383-398.
9. A. Auroux and A. Gervasini, *J. Phys. Chem.*, **1990**, *94*, 6371-6379.
10. L. Zhao, Z. Wang, D. Han, D. Tao and G. Guo, *Mat. Reseach Bull.*, **2009**, *44*, 984-988.
11. Y. Hao, M. Mihaylov, E. Ivanova, K. Hadjiivanov, H. Knözinger and B.C. Gates, *J. Catal.*, **2009**, *261*, 137-149.
12. L.-H. Wang, X.-D. Yi, W.-Z. Weng and H.-L. Wan, *Catal. Today*, **2008**, *131*, 135-139.
13. V. Choque, N. Homs, R. Cicha-Szot and P. Ramirez de la Piscina, *Catal. Today*, **2009**, *142*, 308-313.
14. X. Li-Jin, Q. Fa-Li and L. Shao-Jie, *J. of Natural Gas Chem.*, **1996**, *51*, 126-135.
15. K. Otsuka, Y. Murakami, Y. Wada, A.A. Said and A. Morikawa, *J. of Catal.*, **1990**, *121*, 122-130.